Pramana – J. Phys. (2016) 87: 25
DOI 10.1007/s12043-016-1217-7

End modes in arrays of modulated Su–Schrieffer–Heeger chains

BRAJESH NARAYAN

Amity Institute for Applied Sciences, Amity University, Sector 125, Noida 201 313, India
E-mail: brajesh.n04@gmail.com

MS received 25 December 2014; revised 16 August 2015; accepted 1 October 2015; published online 15 July 2016

Abstract. In this article, an extended and modulated version of the classic Su–Schrieffer–Heeger model is analysed. The nature of the end modes and the effect of cyclic modulation of the hopping parameters are studied in detail. The analysis is extended to the case of an array of linear chains described by the Su–Schrieffer–Heeger model, where the robustness of the end states for a large range of coupling strengths between the chains is found.

Keywords. Su–Schrieffer–Heeger model; topological insulator; tight binding method.

PACS Nos 73.90.+f; 73.20.At; 73.20.−r

1. Introduction

In the past few years, the topological aspects of condensed matter physics have emerged at the forefront of research. With the recent discovery of topological insulators [1,2], a number of lattice models have been revisited in the context of their topological nature. The Su–Schrieffer–Heeger (SSH) model, originally proposed to describe polyacetylene chains [3], is one such simple case. While being straightforward to formulate, it harbours a kaleidoscope of interesting features, including solitons and topological edge modes. Recently, the extended SSH model, including next-nearest neighbour interactions, was studied with a cyclic modulation of the hopping strengths [4]. Intriguingly, this extended SSH model was found to show a topological phase diagram identical to Haldane's model [5]. While Haldane's model is formulated in two spatial dimensions, in the case of one-dimensional extended SSH model the modulation parameter plays the role of the second momentum.

Motivated by this recent development, in the present paper, the modulated Su–Schrieffer–Heeger (mSSH) model for a wide range of Hamiltonian parameters has been systematically studied and the nature of eigenvalues and eigenmodes mapped out. The analysis is then extended to the case of an array of mSSH chains which are coupled together, analogous to a bundle of polyacetylene linear chains, and how the nature of edge modes changes as the coupling strength between the chains is varied, is shown.

2. Model

Let us consider the following Hamiltonian:

$$H = H_{\mathrm{SSH}} + H_{\mathrm{NNN}}, \tag{1}$$

where

$$H_{\mathrm{SSH}} = \sum_n (t_1 c^\dagger_{\mathrm{A},n} c_{\mathrm{B},n} + t_2 c^\dagger_{\mathrm{A},n+1} c_{\mathrm{B},n}) + \mathrm{h.c.} \tag{2}$$

and

$$H_{\mathrm{NNN}} = \sum_n (t_{\mathrm{A}} c^\dagger_{\mathrm{A},n} c_{\mathrm{A},n+1} + t_{\mathrm{B}} c^\dagger_{\mathrm{B},n} c_{\mathrm{B},n+1}) + \mathrm{h.c.} \tag{3}$$

In the above, $t_1 = t(1 + \delta\cos\theta)$ and $t_2 = t(1 - \delta\cos\theta)$, with δ representing the dimerization strength and θ representing a cyclical parameter which can vary from 0 to 2π continuously. The operators $c_{n,\mathrm{A}}$ (or $c_{n,\mathrm{B}}$) are the annihilation operators localized on site A (or B) of the nth cell, and t_{A} and t_{B} are the next-nearest neighbour (NNN) hopping amplitudes along sublattices A and B, respectively. Here and henceforth, $t = 1$ is set as the unit of energy.

If one has a periodic system, Fourier transformation can be used to solve the energy spectrum, such that $c_{\alpha,n} = 1/\sqrt{N}\sum_k \mathrm{e}^{ikn} c_{\alpha,k}$, where N is the number of

unit cells, α corresponds to the site A or B and k is the crystal momentum. The Hamiltonian can then be rewritten in the form

$$H = \psi_k^\dagger h(k) \psi_k, \tag{4}$$

where

$$\psi_k^\dagger = (c_{\mathrm{A},k}^\dagger, c_{\mathrm{B},k}^\dagger)$$

and

$$h(k) = \begin{bmatrix} 2t_\mathrm{A}\cos k & t_1 + t_2\exp(-ik) \\ t_1 + t_2\exp(-ik) & 2t_\mathrm{B}\cos k \end{bmatrix}. \tag{5}$$

The eigenenergies and wavefunctions of the system are then obtained by the diagonalization of the above Hamiltonian. The energy levels are obtained in the straightforward manner as

$$E(k) = (t_\mathrm{A} + t_\mathrm{B})\cos k \pm \sqrt{(t_\mathrm{A} - t_\mathrm{B})^2\cos^2 k + t_1^2 + t_2^2 + 2t_1 t_2 \cos k}. \tag{6}$$

If the system is not periodic, then one needs to use the original Hamiltonian defined in real space and the spectrum can be obtained by a numerical diagonalization of the Hamiltonian matrix.

3. Results and discussion

First we calculate the energy values for the mSSH model by considering only the nearest-neighbour hopping in a chain with 100 sites using open boundary conditions. This is shown in figure 1A, where one can note the existence of a zero mode for θ values ranging from $\pi/2$ to $3\pi/2$. This doubly-degenerate state is completely flat and matches with numerous previous investigations of the SSH model. The existence of this zero mode in the SSH model is protected by inversion symmetry and particle–hole symmetry. To study the effect of breaking this symmetry, the NNN hopping term is next introduced in the problem. The resulting energy spectra for different parameter values of t_A and t_B are shown in figures 1B–1D. Introducing such NNN terms has multiple effects, removing the positive-to-negative energy symmetry of the spectrum (particle–hole symmetry breaking), lifting the degeneracy of the zero mode and removing the flatness of the mode. When $t_\mathrm{A} = t_\mathrm{B}$ (figure 1B), for nonzero value of NNN hopping, the E–θ graph obtained is not symmetric about zero energy. Here particle–hole symmetry is not satisfied, whereas we have the degeneracy of the edge modes as inversion symmetry is still preserved. Next, for $t_\mathrm{A} = -t_\mathrm{B}$, a gap in the energy spectrum opens up and we obtain two different branches of edge modes. On modulating the parameter θ, the two branches of edge modes do not have crossing and do not connect the separate bands. This behaviour persists when t_A and t_B have different magnitudes (see figure 1D).

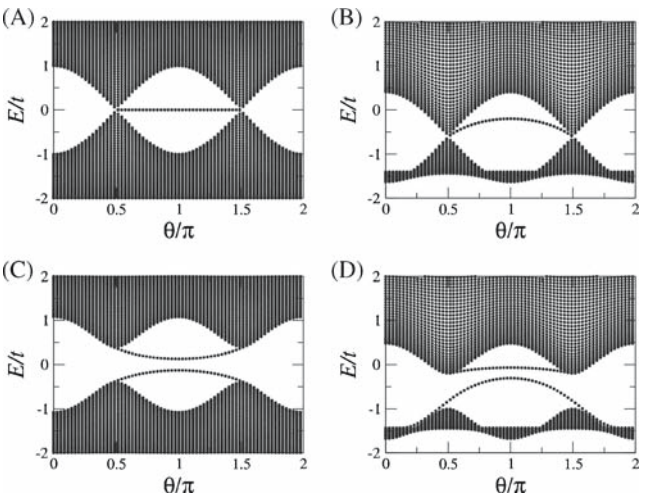

Figure 1. Energy spectrum for the extended SSH model with 100 sites and $\delta = 0.5$ for (**A**) $t_\mathrm{A} = t_\mathrm{B} = 0$, (**B**) $t_\mathrm{A} = t_\mathrm{B} = 0.3$, (**C**) $t_\mathrm{A} = -t_\mathrm{B} = 0.2$ and (**D**) $t_\mathrm{A} = 0.5$, $t_\mathrm{B} = 0.1$.

Till now the NNN hopping term was fixed to a constant value, i.e., it was not varying with θ. The modulation was present only in NN term, i.e., it was varying with θ. Now, to obtain topologically nontrivial properties, the modulation of NNN hopping with θ is also included. This NNN term, after considering modulation, is given by

$$t_\mathrm{A} = h\cos(\theta + \phi), \quad t_\mathrm{B} = h\cos(\theta - \phi). \tag{7}$$

Here h is the parameter which controls the NNN hopping amplitude. Different values of ϕ have been chosen to get symmetric or antisymmetric NNN term. One can notice that the edge mode spectrum exhibits similar characteristics except for $\phi = 0$. For all values of ϕ, except $\phi = 0$, edge modes cross each other and connect the separate bands, unlike the previous case when we did not modulate the NNN terms. Even on continuously varying the parameter θ, the two edge modes cross each other and connect the bulk spectra, suggesting that it represents a topologically nontrivial state. For $\phi = -\pi/4$ and $\pi/4$, bulk spectra are the same but edge modes are located on opposite sides (see figures 2A–2C). When $\phi = 0$, the two branches of edge modes merge to give single band and the two bulk spectra also touch each other (see figure 2B). These features have also been previously studied by Li *et al* [4], and our results match theirs, except for the discrepancy in the wavefunction of the edge mode for $\phi = 0$.

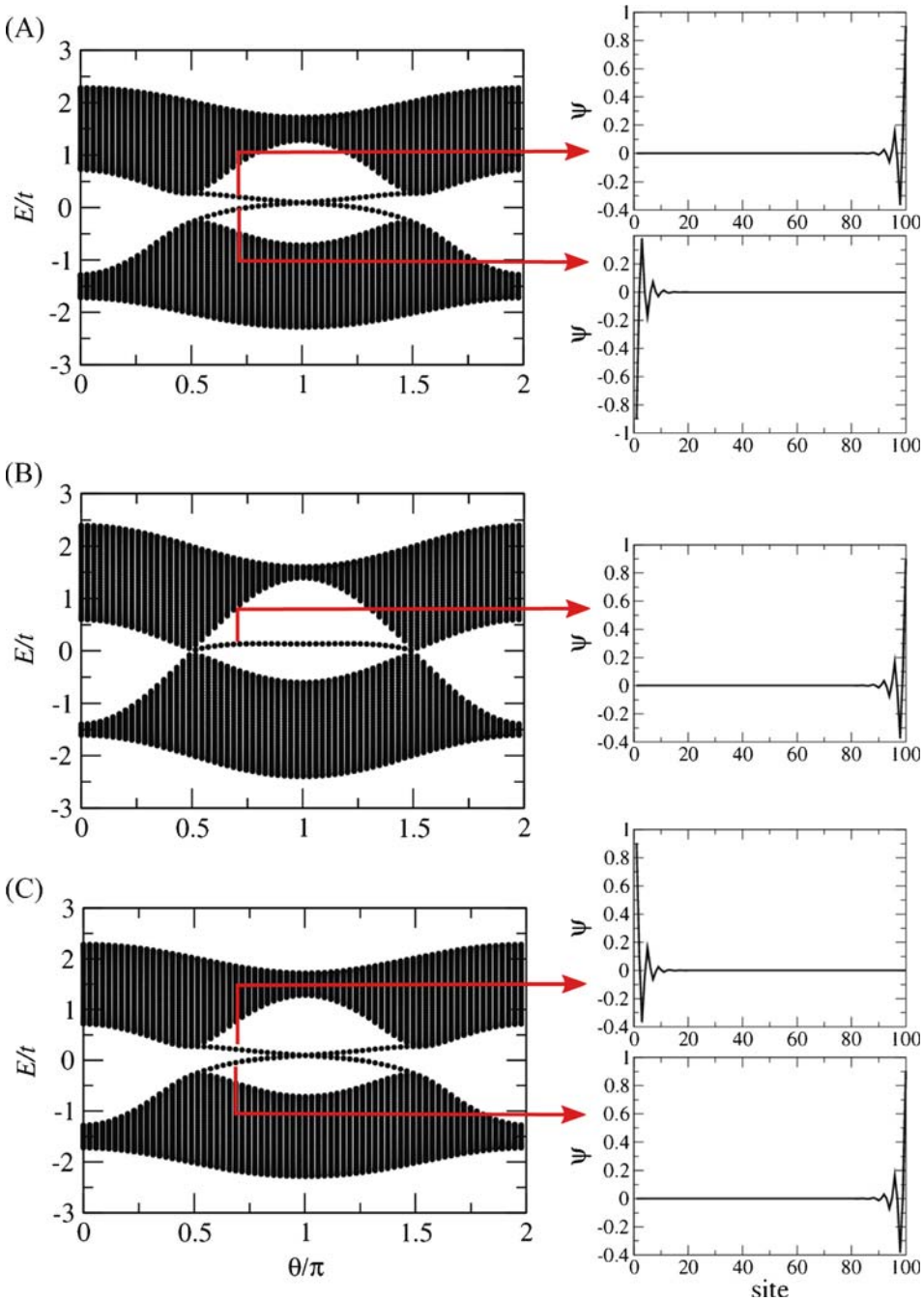

Figure 2. Energy spectrum for the extended SSH model with 100 sites and $\delta = 0.5$ and $h = 0.2$. (**A**) $\phi = -\pi/4$, (**B**) $\phi = 0$, (**C**) $\phi = \pi/4$. For $\phi = 0$, $t_A = t_B$ and the two branches of the edge modes merge together. Graphs **A** and **C** are identical and only their wavefunction is in opposite direction.

The results reported in the above were known and we have reproduced them here. Next, it is interesting to ask what happens when we do not vary all the NNN terms with θ but modulate only some of the terms. So, next we study the SSH model with modulation in only half of the NNN hoppings. For the first 50 sites we have

$$t_A = h\cos(\theta + \phi), \quad t_B = h\cos(\theta - \phi) \tag{8}$$

and for the rest of the sites

$$t_A = X_A, \quad t_B = X_B. \tag{9}$$

For different values of X_A and X_B, and continuously changing values of ϕ, the energy values are calculated. For all values of X_A and X_B, except $X_A = X_B = 0$ and $X_A = -X_B$, edge mode branches do not cross each other and in each of these cases, the bulk spectra touch each other (see figures 3A–3C, 3E–3G, 3I–3K).

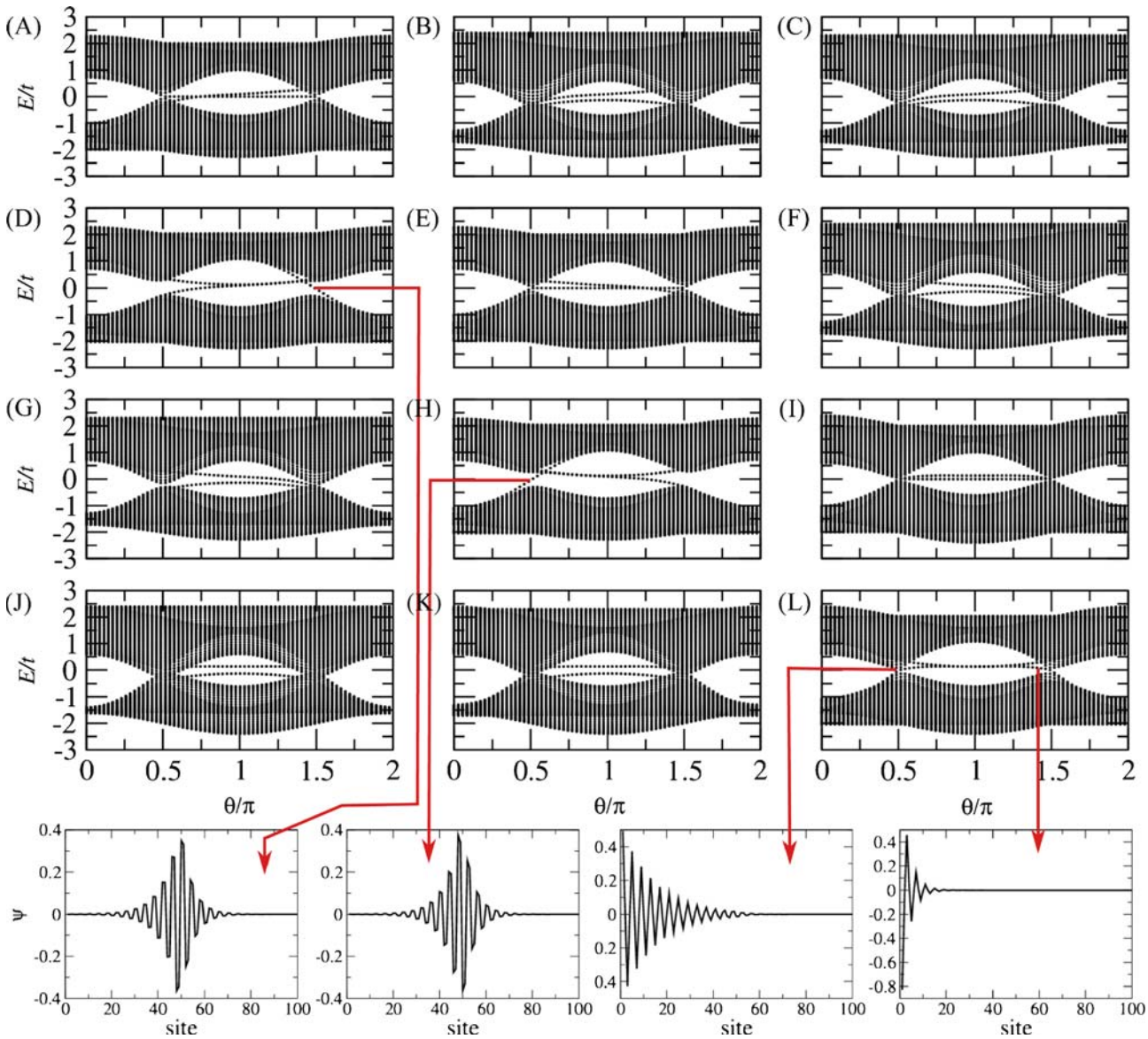

Figure 3. Energy spectrum for the extended SSH model with 100 sites and $\delta = 0.5$ and $h = 0.2$. In (**A**), (**B**), (**C**) and (**D**) $\phi = -\pi/4$; in (**E**), (**F**), (**G**) and (**H**) $\phi = \pi/4$ and in (**I**), (**J**), (**K**) and (**L**) $\phi = 0$. For (**A**), (**E**) and (**I**) $X_A = X_B = 0$, (**B**), (**F**) and (**J**) $X_A = X_B = 0.2$, (**C**), (**G**) and (**K**) $X_A = 0.1$ and $X_B = 0.2$ and (**D**), (**H**) and (**L**) $X_A = -X_B = 0.2$. Wavefunctions of the edge modes, for (**D**), (**H**) and (**L**), has also been shown. Wavefunction of the edge modes of other graphs have similar nature to that of full modulation.

For $X_A = X_B = 0$, the bulk spectra touch each other and the edge mode branches cross each other. The most interesting result is for the condition $X_A = -X_B$ and $\phi \neq 0$. In this case, the bulk spectrum has a gap. The two edge modes cross each other but the edge mode emerging from the lower bulk joins the upper bulk and the other edge mode branch which emerges from the upper bulk also joins the upper branch instead of joining the lower bulk. There is a third branch emerging from the upper bulk which joins the lower bulk crossing the two edge mode branches. The wavefunctions of the edge modes are similar to wavefunctions of the other cases. Also, the wavefunctions of these edge modes are similar to that obtained in fully modulated chain. The nature of wavefunction for this third branch is different from other two branches. To illustrate, as shown in figures 3D and 3H $\phi = -\pi/4$ and $\phi = \pi/4$ were chosen, respectively. The bulk spectrum of both the cases are identical but the third branch and the edge modes are on opposite sides. States with ϕ and states with $-\phi$ are different topological states. Wavefunction for this third branch shows a finite amplitude in the middle of

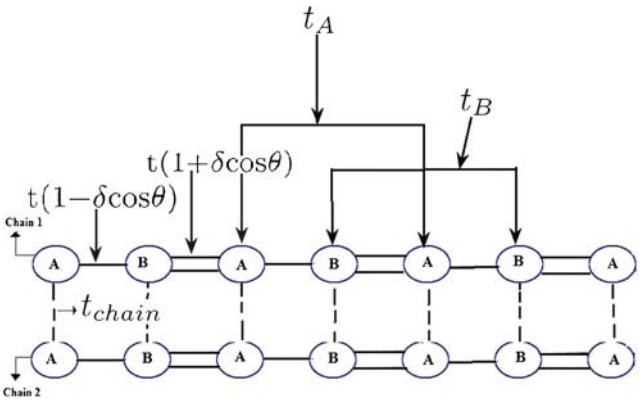

Figure 4. Array of chains of atoms. 'A' represents one kind of atoms and 'B' another kind. The chain is made up of atoms A and B positioned alternately. For NN, hopping coefficient is $t(1-\delta\cos\theta)$ and $t(1+\delta\cos\theta)$ for single and double bond respectively. t_{A} and t_{B} are the hopping coefficient for NNN of A and B. In between the chains, t_{chain} is the hopping coefficient.

the chain for both figures 3D and 3H, suggesting that it is not an edge mode. For no other combination of X_{A}, X_{B} and ϕ investigated in this work, could one obtain such a spectrum. Wavefunction of all the edge modes is similar to that obtained in a chain with all NNN terms modulated.

To study the effect of the presence of other chains and to find if such states are present in arrays of chains, $E-\theta/\pi$ for an array of three chains was next computed. Figure 4 shows an array of two chains. An array of three chains was made by placing an identical chain in the plane of the two chains shown in figure 4 and parallel to them. We assumed hopping coefficient between the chains to be t_{chain} for both A–A and B–B interchain interactions. Initially, an array was made of chains with modulation of all NNN terms. To study this effect, the band structure for various values of t_{chain} and ϕ were generated. Firstly, $t_{\mathrm{chain}} = 0.05$ was fixed. It was observed that the edge mode spectrum exhibits similar characteristics as before, except for $\phi = 0$. Also, for all values of ϕ except $\phi = 0$, edge modes cross each other and connect the separate bulk bands. These represent topologically nontrivial states. For $\phi = -\pi/4$ and $\pi/4$, bulk spectra are identical but edge modes are located on opposite sides. The nature of graphs obtained is the same as that for the single chain. However, the number of branches of edge modes is now enhanced (see figure 5). For each chain there is a pair of edge modes. When $\phi = 0$, the two branches of the edge modes merge to give a single branch, thus we get three branches for an array of three chains. The two bulk spectra also touch each other. Energy spectrum obtained is similar to the energy spectrum of the single chain with all NNN terms varying with θ. The value of t_{chain} was increased to 0.1. Now the gap between the two bulk bands is reduced but the gap between the edge mode branches increases. Still, for $\phi = -\pi/4$ and $\phi = \pi/4$, bulk spectra are identical and the edge mode branches cross each other and connect the bulk bands. For $\phi = 0$, we have three edge mode branches

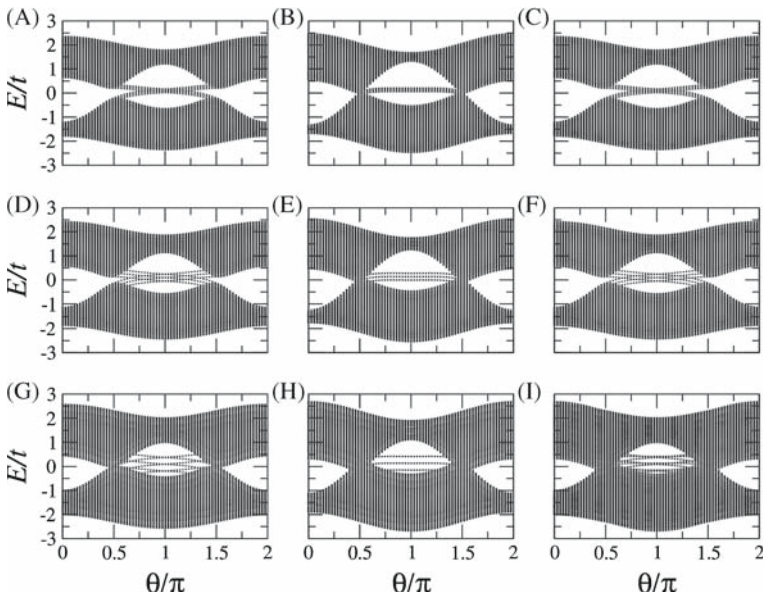

Figure 5. Energy vs. θ/π. For (**A**), (**D**) and (**G**) $\phi = -\pi/4$; (**B**), (**E**) and (**H**) $\phi = 0$; (**C**), (**F**) and (**I**) $\phi = \pi/4$. For (**A**), (**B**) and (**C**) $t_{\mathrm{chain}} = 0.05$; (**D**), (**E**) and (**F**), $t_{\mathrm{chain}} = 0.1$; (**G**), (**H**) and (**I**) $t_{\mathrm{chain}} = 0.2$.

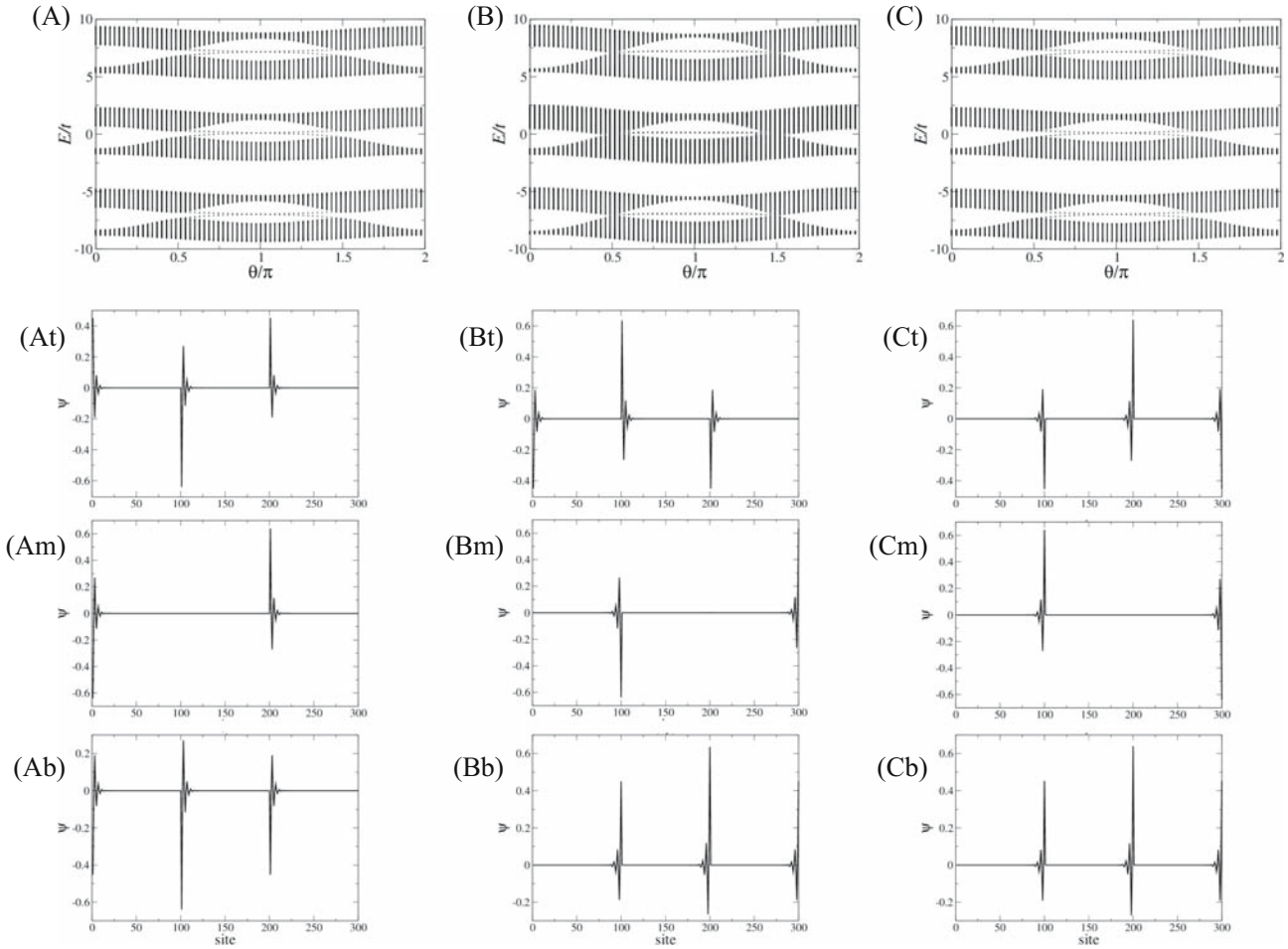

Figure 6. Energy vs. θ/π. For (**A**) $\phi = -\pi/4$; (**B**) $\phi = 0$ and (**C**) $\phi = \pi/4$. For (**A**), (**B**) and (**C**) $t_{\text{chain}} = 5$. A(t), B(t) and C(t) are wavefunctions of the edge modes of the first chain, i.e., top-most energy spectrum of (**A**), (**B**) and (**C**), respectively. Similarly A(m), B(m) and C(m) are edge mode wavefunctions of the second chain and A(b), B(b) and C(b) are the edge mode wavefunctions of the third chain of (**A**), (**B**) and (**C**), respectively.

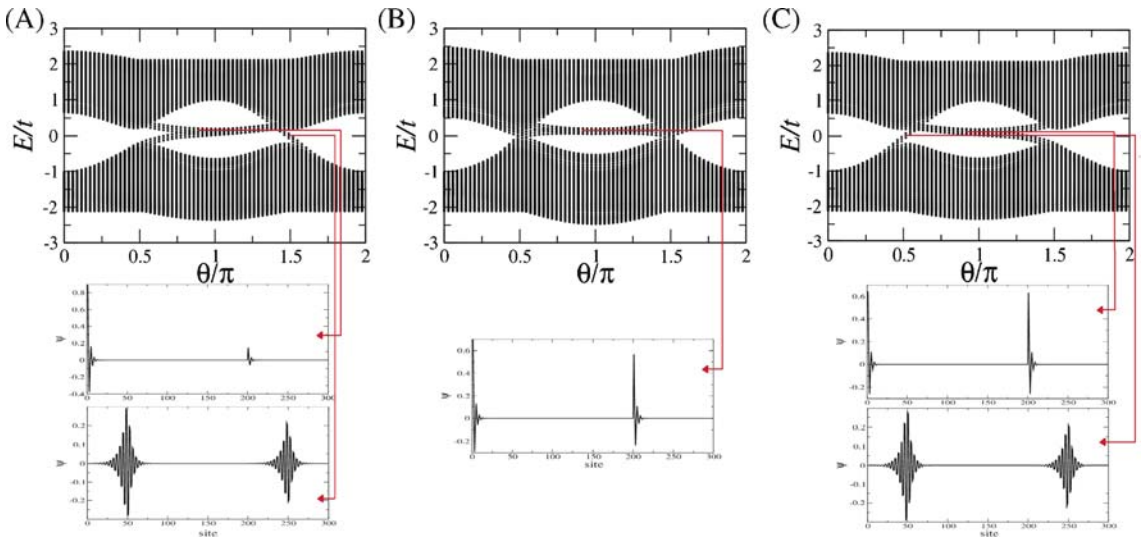

Figure 7. Energy vs. θ/π. For (**A**) $\phi = -\pi/4$; (**B**) $\phi = 0$; (**C**) $\phi = \pi/4$. For (**A**), (**B**) and (**C**) $t_{\text{chain}} = 0.05$ and $X_{\text{A}} = -X_{\text{B}} = 0.2$. Below energy spectra are edge mode wavefunctions of second chain or the middle branch. For $\phi = -\pi/4$ and $\phi = \pi/4$, two wavefunctions are shown, one for the main edge mode branch and the other for the new edge mode on the side.

and the space between each has increased. When the t_{chain} value was increased to 0.2, even for $\phi = -\pi/4$ and $\pi/4$, the bulk spectra joined each other as shown in figure 5. The edge mode branches still cross each other. For $\phi = 0$, the space between the edge mode branches further increased. The nature of wavefunction for the edge modes remained the same even on increasing the value of t_{chain}. Gradually, on increasing the value of t_{chain} a stage is reached when edge mode branch of one chain coincides in energy with the bulk of another chain. At this stage, the wavefunction of this edge mode is not the same as obtained earlier. On further increasing t_{chain}, we are able to obtain energy bands of each chain distinctly. To illustrate this, $t_{\text{chain}} = 5$ was chosen. Figure 6 shows the energy bands and wavefunction of the edge mode branch for each chain. We know that there are two edge modes for each chain and when $\phi = 0$, these are very close (almost overlapping). In the figure, we can see energy band of each chain separately and each is identical to its corresponding single chain energy bands. If we take the first edge mode branch of the first chain and the first edge mode branch of the third chain and plot the wavefunction, then, these are similar as shown for $\phi = -\pi/4$ and $\pi/4$ in figure 6 A(t), A(b) and C(t), C(b). If we chose the first edge mode branch for the first chain and the second edge mode branch for the third chain or vice versa, the disturbance in the wavefunction obtained is on the opposite side as shown for $\phi = 0$ in figure 6 B(t) and B(b). The nature of wavefunction obtained is similar to the corresponding single-chain wavefunction and the only difference is that these are repeated three times (one after the other) as there are three chains in the array. The wavefunction for the second branch, i.e., the one in the middle, is different from that obtained for the first and third chain. It is not a repetition of wavefunction of the corresponding single chain thrice. There are only two enhanced amplitudes rather than three, one for the first chain and other for the third, either at the beginning of each chain or at the end of chains (see figure 6, A(m), B(m) and C(m)).

Next, we study array of chains with modulation of half of NNN terms of each chain of the array. Nature of all the graphs is similar to the graph for the single chain, apart from the fact that there is an increase in the number of edge mode branches. The spectrum is shown in figure 7 for $X_{\text{A}} = -X_{\text{B}}$ and $t_{\text{chain}} = 0.05$. We can see that even the number of third branch connecting upper bulk band to lower, in $\phi = -\pi/4$ and $\phi = \pi/4$ increases (see figure 7). One branch of each chain, i.e., number of the third branch is equal to the number of chains in the array. We can notice that for $\phi \neq 0$, bulk bands are not connected and an edge mode branch emerges from the upper bulk to join the upper bulk again. Edge mode branch from the lower bulk joins the upper bulk. On changing $\phi = 0$, the gap between the upper and lower bulk band disappears. Here too we notice that the gap between the bulk bands decreased and gap between the edge mode branches increased with increase in t_{chain} value. Similar deviations and similarities from the corresponding single chain, as well as for array of chains with modulations in all NNN terms was also observed. This is also true for the new set of edge mode branches obtained on the side. Figure 7 shows wavefunctions of the edge mode of the second chain. Even for the new edge mode branch, there are only two peaks in the wavefunction of the second chain.

For the same array, modulation in t_{chain} for half the array was added.

$$t_{\text{chain}} = (T_{\text{chain}}) \cos(\theta + \phi), \tag{10}$$

where $T_{\text{chain}} = 0.05$. For the rest, $t_{\text{chain}} = 0.05$. The energy spectrum is similar to the spectrum of single chain with half modulation. Now the number of edge mode branches and the number of third branch increased.

4. Conclusions

In the end, we can conclude that energy spectra for single-chain and multiple Su–Schrieffer–Heeger chains are similar. Topologically, nontrivial states for single-chain and multiple chains are similar for mSSH models with a modulation in half of the chain as well as in the whole chain. Also notable is the robustness of the end states for large range of coupling strengths between the chains.

Acknowledgements

The author would like to acknowledge Dr Awadhesh Narayan for suggesting this problem.

References

[1] M Z Hasan and C L Kane, *Rev. Mod. Phys.* **82**, 3045 (2010)
[2] X-L Qi and S-C Zhang, *Rev. Mod. Phys.* **83**, 1057 (2011)
[3] W P Su, J R Schrieffer and A J Heeger, *Phys. Rev. Lett.* **42**, 1698 (1979)
[4] L Li, Z Xu and S Chen, *Phys. Rev. B* **89**, 085111 (2014)
[5] F D M Haldane, *Phys. Rev. Lett.* **61**, 2015 (1988)